Revista Mexicana de Física
ISSN: 0035-001X
rmf@ciencias.unam.mx
Sociedad Mexicana de Física A.C.
México

Pérez, E.; Gomez-Polo, C.; Larumbe, S.; Pérez-Landazabal, J.I.; Sagredo, V.
Structural and magnetic properties of NiFe2 O4 and NiFe2 O4 /SiO2 nanoparticles prepared by Sol-Gel combustion
Revista Mexicana de Física, vol. 58, núm. 2, diciembre, 2012, pp. 104-107
Sociedad Mexicana de Física A.C.
Distrito Federal, México

Revista Mexicana de Física S **58** (2) 104–107 DICIEMBRE 2012

Structural and magnetic properties of $NiFe_2O_4$ and $NiFe_2O_4/SiO_2$ nanoparticles prepared by Sol-Gel combustion

E. Pérez[a], C. Gomez-Polo[b], S. Larumbe[b], J.I. Pérez-Landazabal[b], and V. Sagredo[a,*]
[a]*Laboratorio Laboratorio de Magnetismo, Departamento de Física, Facultad de Ciencias, Universidad de Los Andes, Mérida-Venezuela.*
[*]*e-mail: sagredo@ula.ve*
[b]*Departamento de Física, Universidad Pública de Navarra, Campus de Arrosadia, E-31006 Pamplona- Spain.*

Recibido el 25 de junio de 2010; aceptado el 9 de octubre de 2010

$NiFe_2O_4$ nanoparticles have been prepared by sol-gel autocombustion technique, some of them have been supported in SiO_2 following the TEOS technique. Particle formation and structural and magnetic properties were investigated by using X-ray diffraction, scanning electron microscopy (SEM) and magnetization measurements. SEM characterization shows a more ordered array of $NiFe_2O_4$ nanoparticles in silica matrix. Besides that, magnetization measurements as a function of temperature indicated a lower dipole-dipole interactions in this sample. The magnetization data as a function of magnetic field suggest some surface modification on the nanoparticles.

Keywords: Magnetite; angustifolia kunth bamboo; magnetization; in-situ co-precipitation; Spinel; nanoparticles.

Nanopartículas de $NiFe_2O_4$ han sido preparadas mediante la técnica de sol-gel-auto combustión, alguna de ellas han sido soportadas en SiO_2 siguiendo la técnica de usar TEOS. La formación de las partículas y las propiedades estructura les y magnéticas fueron investigadas mediante difracción de rayos-X, microscopía electrónica de barrido (SEM) y medidas de magnetización. La caracterización por SEM muestra un arreglo más ordenado de las partículas de $NiFe_2O_4$ en la matriz de SiO_2. Además las mediciones de magnetización en función de la temperatura indican la presencia de interacciones dipolo-dipolo más débiles que la muestra sin SiO_2. Los resultados de la magnetización en función del campo magnético sugieren cierta modificación en la superficie de las partículas.

Descriptores: Nanopartículas; angustifolia; magnetización.

PACS: 61.05cp; 75.50

1. Introduction

Nanophase spinel ferrite particles have attracted considerable attention owing to their technological importance in the application areas, such as microwave devices-microwave absorbers and waveguides in the gigahertz region, high speed digital tape and disk recording, repulsive suspension for use in levitated systems, ferrofluids, catalysis, and magnetic refrigeration systems [1,2]. Nanocrystalline ferrites are potential materials for biomedical application as a magnetic carrier for drug delivery [3].

Due to the significant surface-to-volume ratio, anomalous magnetic behaviors, derived from surface spin disorder, have been observed in mechanically activated $NiFe_2O_4$ nanoparticles [4,5].

Among the different ferrites, which form a major constituent of magnetic ceramic materials, spinels of the type AB_2O_4 such as: $MnFe_2O_4$, $NiFe_2O_4$ and $CoFe_2O_4$ have attracted considerable attention due to their wide applications in several technological fields [6]. $NiFe_2O_4$ is a typical soft ferromagnetic material, which crystallizes in a completely inverse spinel structure with all nickel ions located in the octahedral sites and iron ions occupying tetrahedral and octahedral sites [7]. The spinel structure contains two cation sites for metal cation occupancy. There are 8 A-sites in which the metal cations are tetrahedrally coordinated with oxygen, and 16 B-sites which possess octahedral coordination. When the A-sites are occupied by Me2+ cations and the B-sites are occupied by Fe^{3+} cations, the ferrite is called a normal spinel. If the A-sites are completely occupied by Fe^{3+} cations and the B sites are randomly occupied by Me^{2+} and Fe^{3+} cations, the structure is referred to as an inverse spinel [8,9].

We present here the study of nanoparticles of $NiFe_2O_4$prepared by two different methods, sol-gel autocombustion and nanocomposites of nickel ferrite in silica support.

2. Experimental

In order to study the influence of the preparation method on the structural and magnetic properties of nickel ferrite nanoparticles we have prepared nanoparticles by using sol gel autocombustion process and nanocomposites of nickel ferrite in silica support. The silica matrix was used not only to serve as spatial nucleation sites, but 1 also to confine the coarsening of nanoparticles and minimize the degree of crystalline aggregation. Because it is well known that magnetic nanoparticles tend to agglomerate, not only because of their large surface energy, but also because of their strong magnetic interactions [10,11].

Two samples $(NiFe_2O4)_x$ $(SiO_2)_{1-x}$ with x= 100 and 40 wt% were synthesized by using sol-gel autocombustion method. Several chemical processing techniques have been investigated to prepare ultrafine powders. Among these tech-

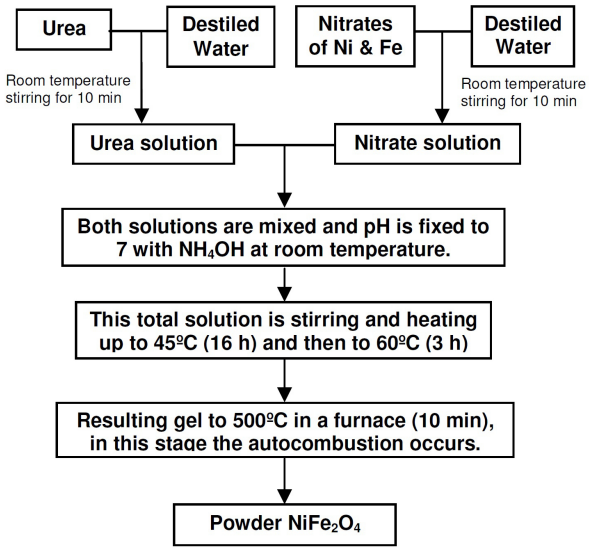

FIGURE 1. Flow chart showing the synthesis of $NiFe_2O_4$ nanoparticles by sol-gel autocombustion method.

iques, combustion synthesis has been proved to be simple and nonexpensive [12]. The flow chart used for preparing nanosized nickel ferrite powders is shown in Fig. 1.

The precursor solutions were prepared by dissolving Fe and Ni nitrates in deionized water plus urea as fuel. After continuous stirring the pH was adjusted to 7, the solutions were allowed to gel by continuous heating for 19 hrs. After all that procedure, the gel was submitted to thermal treatment at 500°C in a preheated furnace where the combustion process was developed.

For the sample supported in SiO_2 a silica precursor, tetraethoxysilane (TEOS) in ethanol was added to the nitrate solution. After about 6 h of stirring and heating the ethanol evaporation and the evolution of TEOS hydrolysis and condensation reaction was obtained then the obtained gels were introduced in a preheated furnace up to the autocombustion reaction occurred.

3. Characterizacion

The obtained samples were characterized by powder X.ray diffraction (XDR) and scanning electron microscopy (SEM). Their magnetic properties were investigated by using a SQUID (MPMS) magnetometer and a vibrating sample magnetometer.

Figure 2 shows the XRD spectra for both type of samples. All the diffraction peaks in Fig. 1a confirmed the formation of the pure single phase spinel nickel ferrite with the face-centered cubic spinel phase with lattice parameter a=8.347 Å. It showed that Ni-ferrite sample was synthesized successfully under sol-gel autocombustion method with urea as fuel.

The Fig. 2b presents very broad peaks attributed to the amorphous nature of the SiO_2 matrix. This results suggest that the xerogel is amorphous.

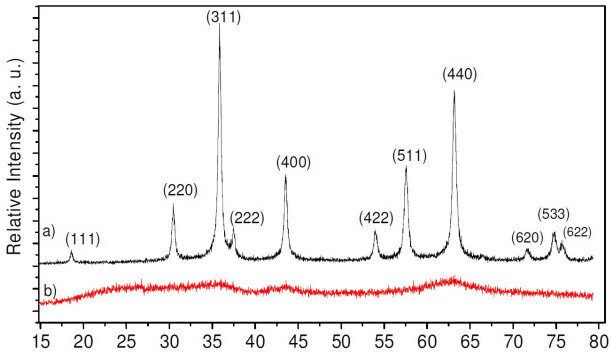

FIGURE 2. XDR patterns of the $(NiFe_2O_4)_x$ $(SiO_2)_{1-x}$ prepared by a) sol-gel autocombustion and b) sol-gel autocombustion/SiO_2.

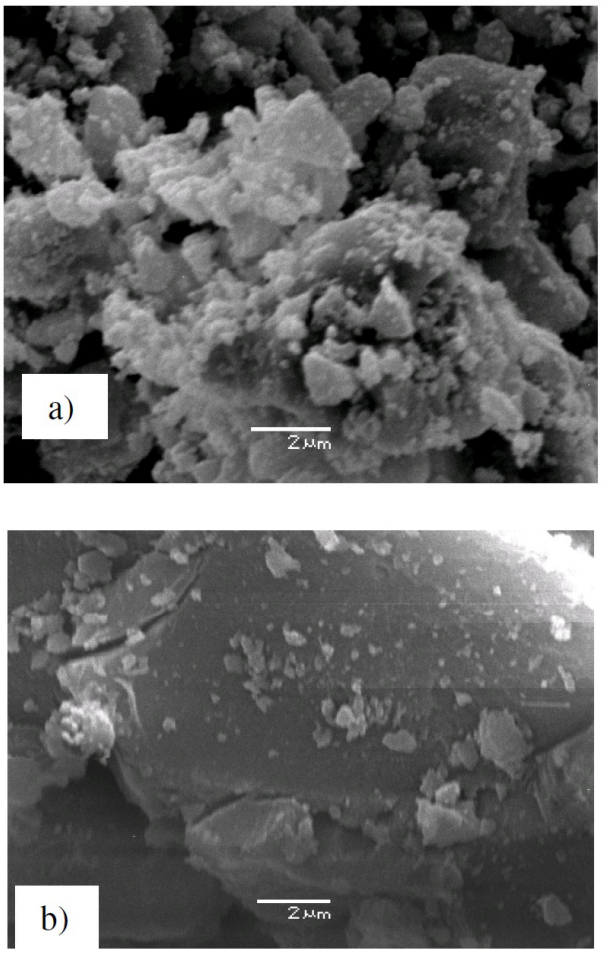

FIGURE 3. Scanning electron micrographs of samples $(NiFe_2O_4)_x$ $(SiO_2)_{1-x}$ prepared by methods a) and b).

The Fig. 2b presents very broad peaks attributed to the amorphous nature of the SiO_2 matrix. This results suggest that the xerogel is amorphous.

SEM images of the $(NiFe_2O_4)_x$ $(SiO_2)_{1-x}$ with x=100 and 40 % are shown in Fig. 3. The differences in morphology among the two samples are clearly shown.

In Fig. 3a, it is possible to notice that the 1 nickel ferrites nanoparticles prepared by sol-gel autocombustion method presents many pores in the gel structure. The formation of the porous network structure may be originated from the liberation of gasses during the combustion process.

Figure 3b shows an image of composite $NiFe_2O_4$ (60%wt SiO_2) where the backscattered electrons show white regions corresponding to the presence of nickel ferrite particles [13]. The darker regions are formed by SiO2 where the ferrite particles are dispersed in the SiO2 matrix presenting a sheet-like morphology. Unfortunately we were not able to estimate the weight factor 40/60 between the nickel ferrite and the composite in this particular observed area.

4. Results and discussion

The magnetic properties for samples a) and b), were studied by using the zero field cooled (ZFC) and field cooled (FC) protocol shown in Fig. 4. For the ZFC experiment, a sample is cooled from room temperature down to 5 K, with no magnetic field on and then heated in a small field (50 Oe) while the net magnetization of the sample is recorded. The FC data are produced by cooling particles in a small field after the ZFC experiment and recording the change in net sample magnetization with temperature. The ZFC data shows a maximum value around room temperature. This maximum is currently associated to the mean blocking temperature of the nanosystem [14].

The FG-1 and FG-4 samples did not display saturation at H=27 kOe, this is due to the nanoparticles of magnetite hosted in the fibers, as these present a superparamagnetic behavior and the saturation field is around H = 50 kOe [15].

The temperature corresponding to this maximum is the temperature at which the relaxation time of the magnetization equals the characteristic time of measurements. It is interesting to notice the differences in the magnetic behavior for the low temperature region for both samples [15]. According to these ideas the magnetic state below the maximum temperature is an ordered state, in this case a ferrimagnetic state.

The hysteresis loop for a sample prepared by the sol-gel autocombustion method was measured to determine parameters as the saturation magnetization (Ms), remnant magnetization (Mr) and coercitivity (Hc) as shown in Fig. 5. In this figure the insert shows the low magnetic field zone in order to observe the shift presented for the coercitive field and the remnant magnetization.

It is evident from that figure that the Ms was not obtained because at 50 KOe the magnetization is still increasing, so the maximum magnetization was about 1.69 mB. The value of Mr is about 0.30 mB and the coercitivity presents some shift to the negative magnetic field scale. The isothermal magnetization was measured at 5 K up to 5 T for sample prepared by sol-gel autocombustion method (b). It can be seen the existence of coercitivity with an average value of 115 Oe. It is important to notice, in both samples, the different behavior of the magnetization in the range of low temperature.

The sol-gel autocombustion sample presents a typical ZFC magnetic behavior at temperatures below the blocking temperature: At the start of the ZFC cycle the magnetic moment of each atom is randomly frozen to an easy axis of the particle and allows them to align with the applied magnetic field increasing the magnetization [14] Instead the FC curve presents a magnetic behavior very influenced by the presence of particle-particle interactions which stabilized the magnetic moments in their original configuration preventing alignment. Concerning with the shape of data M(T) obtained for the $NiFe_2O_4/SiO_2$ sample (b) composite it can be noticed a quite different magnetic behavior. Thus for the FC data we could suggest a reduction in the interparticle interactions which produces an increase in the net magnetization [15]. It is also possible to notice a significant difference between the magnitude of the data for both samples, sample (a) has a magnetization almost two order of magnitude larger than

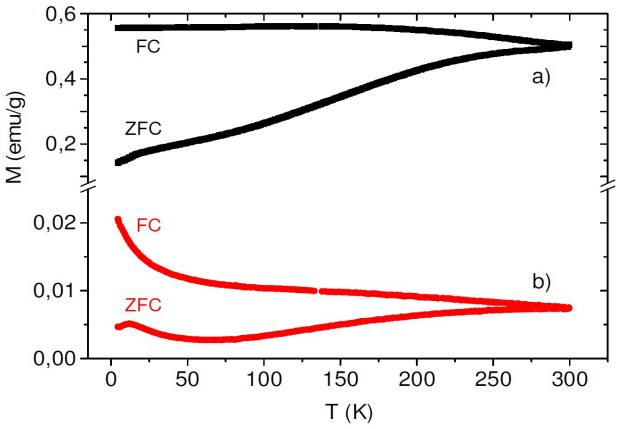

FIGURE 4. Temperature dependence of magnetization for zero field-cooled (ZFC) and field cooled (FC) for $NiFe_2O_4$, nanoparticles prepared by sol-gel autocombustion (a) and sol-gel autocombustion/SiO_2 (b).

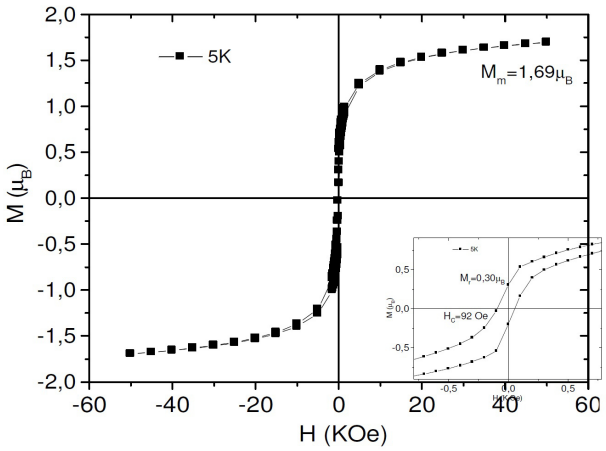

FIGURE 5. Field dependent magnetization hysteresis of nanoparticles of $NiFe_2O_4$, prepared by sol.gel autocombustion sample (a).

sample (b). We assume that the non complete crystallinity suggested by X.ray data is the main fact for that difference.

5. Conclusions

Summarizing the above experimental results we can conclude that the gels can burn in a self-propagating combustion way. After combustion, the gel without SiO2 directly transform into single phase. The dispersion of $NiFe_2O_4$, nanoparticles in a silica matrix through sol-gel autocombustion method allows to obtain assemblies of fairly weak interacting particles. However the $NiFe_2O_4$, nanoparticles prepared by sol-gel autocombustion method without SiO_2 present a fairly high magnetization under high applied magnetic field, very close to the theoretical 2 mB for the inverse spinel structure. A significant shift in the coercitive field was observe for this sample in the hysteresis loop taken at 5 K. Further work should be necessary to give a valid explanation for this effect.

Acknowledgements

The financial support of Research Projects CDCHT-ULA, C-1624-08-05-ED and C-1658-09-05-A is gratefully acknowledged for the authors V.Sagredo and E.Perez.

1. Q.A. Pankhurst, J. Conolly, S.K. Jones, and Dobson, *J. Phys D.* **36** (2003).
2. A.H. Lu, W.C. Li, N. Matoussevitch, B. Spliethoff, H. Bonnemann, and F. Schuth, *Chem Commun.* **23** (2005) 98.
3. M. Latorre-Esteves, M. Cortes Torres-Lugo, and C. Rinald, *Journal of Magnetism and Magnetic Materials* **321** (2009) 3061.
4. R.H. Kodama, *Journal of Magnetism and Magnetic Materials* **200** (1999) 359.
5. J. Nogues, Ivan K. Schuller, *Journal of Magnetism and Magnetic Materials **192** (1999)203.*
6. S. Mitra, K. Mandal, and P. Anil Kumar, *Journal of Magnetism and Magnetic Materials* **306** (2006) 254.
7. D.S. Mathew and R.S. Juang, *Chem. Eng. J.* (2006) doi:10.1016/j.cej.2006.11.001.
8. C.R. Vestal and J.Z. Zhang, *Int. J. Nanotechnol.* **1** (2004) 240.
9. L. Neel, *Ann. Phys. Paris* **3** (1948) 137–198.
10. Z.H. Zhou, J.M. Xue, J. Wang, H.S. Chan, T. Yu, and Z.X. Shen, *Journal of Applied Physics* **91** (2002) 6015.
11. C. Cannas, A. Musinu, D. Peddis, and G.G. Piccaluga, *Chem. Matter* **18** (2006) 3835.
12. M. Knobel, L.M. Socolovsky, and J.M. Vargas, *Rev. Mex. Fis. E* **50** 8–28.
13. Z. Yue, W. Guo, J. Zhou, Z Gui, L. Li, *Journal of Magnetism and Magnetic Materials* **270** (2004) 216.
14. C. Cannas, A. Musinu, G. Piccaluga, D. Fiorani, D. Peddis, H. Rasmussen, and S. Morup, *Journal of Chem Phys.* **125** (2006) 164714.
15. A. Gross, M. Dichl, K. Berverly, E. Richman, and L. Tobert, *Phys. Chem.* **107** (2003) 5475.